MOLECULAR AND CELLULAR BIOLOGY, Jan. 2001, p. 354–366 Vol. 21, No. 1
0270-7306/01/$04.00+0 DOI: 10.1128/MCB.21.1.354–366.2001

Translational and Structural Requirements of the Early Nodulin Gene *enod40*, a Short-Open Reading Frame-Containing RNA, for Elicitation of a Cell-Specific Growth Response in the Alfalfa Root Cortex

CAROLINA SOUSA,[1]† CHRISTINA JOHANSSON,[1]‡ CELINE CHARON,[1] HAMID MANYANI,[1] CHRISTOF SAUTTER,[2] ADAM KONDOROSI,[1,3]* AND MARTIN CRESPI[1]

Institut des Sciences Végétales, Centre National de la Recherche Scientifique, F-91198 Gif-sur-Yvette Cedex, France[1]; Institute of Plant Sciences, Swiss Federal Institute of Technology, CH-8092 Zürich, Switzerland[2]; and Institute of Genetics, Biological Research Center, Hungarian Academy of Sciences, H-6701 Szeged, Hungary[3]

Received 29 June 2000/Returned for modification 3 August 2000/Accepted 3 October 2000

A diversity of mRNAs containing only short open reading frames (sORF-RNAs; encoding less than 30 amino acids) have been shown to be induced in growth and differentiation processes. The early nodulin gene *enod40*, coding for a 0.7-kb sORF-RNA, is expressed in the nodule primordium developing in the root cortex of leguminous plants after infection by symbiotic bacteria. Ballistic microtargeting of this gene into *Medicago* roots induced division of cortical cells. Translation of two sORFs (I and II, 13 and 27 amino acids, respectively) present in the conserved 5′ and 3′ regions of *enod40* was required for this biological activity. These sORFs may be translated in roots via a reinitiation mechanism. In vitro translation products starting from the ATG of sORF I were detectable by mutating *enod40* to yield peptides larger than 38 amino acids. Deletion of a *Medicago truncatula enod40* region between the sORFs, spanning a predicted RNA structure, did not affect their translation but resulted in significantly decreased biological activity. Our data reveal a complex regulation of *enod40* action, pointing to a role of sORF-encoded peptides and structured RNA signals in developmental processes involving sORF-RNAs.

RNAs encoding only short open reading frames (sORF-RNAs) have received considerable attention in recent years because they show a striking diversity in many cell types from various organisms. Several RNAs exhibit a function without being translated into proteins, for example, tRNAs, rRNAs, RNAs in ribozymes, and small nuclear RNAs from spliceosomes (reviewed in reference 8). However, a pentapeptide-encoding sORF present in the 23S rRNA from *Escherichia coli* was recently shown to render this bacterium resistant to a specific antibiotic (40). In eukaryotes, several sORF-RNAs are induced at specific stages of development, suggesting their participation in various differentiation processes (7, 14, 18, 31, 38, 40, 44, 46). Eukaryotic cells may use sORF-RNAs for the regulation of several cellular processes, as suggested by a thorough analysis of the yeast genome leading to identification of several new noncoding and sORF-containing RNAs (31). In eukaryotes, sORFs present in mRNAs are likely to be translated, since translation of mRNAs is achieved by a scanning mechanism in a 5′-to-3′ direction. Indeed, there are several examples where translation of upstream sORFs regulates expression of the 3′ ORF corresponding to the gene product (15, 43). At the same time, very little is known about the fate of the encoded oligopeptides in the cell and whether translation of sORFs present in sORF-RNAs is relevant for gene activity. For example, even though a putative protein product of the *H19* RNA was detected using immunological approaches (23), the main function of *H19* seems to lie in the mRNA molecule rather than in the encoded protein (24).

Leguminous plants have the ability to enter into symbiosis with N_2-fixing bacteria (collectively called rhizobia) to form the root nodule. Development of this symbiotic organ depends on the coordinate expression of plant and bacterial genes and starts with the induction of root cortical cell divisions (38). The early nodulin gene *enod40* is rapidly induced by rhizobia in the root pericycle and then in the dividing cortical cells of the nodule primordium (1, 12, 21, 45). The *enod40* genes are highly conserved in various leguminous species and have also been found in tobacco and rice (22, 42). They lack a common long ORF, and computer predictions suggest that they code for structured RNAs (12). In the *enod40* genes, two highly conserved regions were distinguished: box I in the 5′ end, spanning a conserved sORF (sORF I), and box II in the central part of the gene (42) (Fig. 1A). We demonstrated that under nitrogen-limiting conditions overexpression of *Medicago truncatula* (a model leguminous plant) *enod40* (*Mtenod40*) induces cortical cell division in *Medicago* roots (9). These experiments also showed that transient expression of either region 1 carrying box I or a 3′ sequence (region 2) spanning box II evoked a response similar to that evoked by the complete gene in alfalfa (*Medicago sativa*) roots.

In order to gain insight into the molecular mechanism of *enod40* action, we used microtargeting to introduce different

* Corresponding author. Mailing address: Institut des Sciences Végétales, Centre National de la Recherche Scientifique, F-91198 Gif-sur-Yvette, France. Phone: 33-1-69823696. Fax: 33-1-69823695. E-mail: Adam.Kondorosi@isv.cnrs-gif.fr.

† Present address: Department of Microbiology and Parasitology, University of Seville, 41080 Seville, Spain.

‡ Present address: Department of Molecular and Structural Biology, Aarhus University, DK-8000 Aarhus, Denmark.

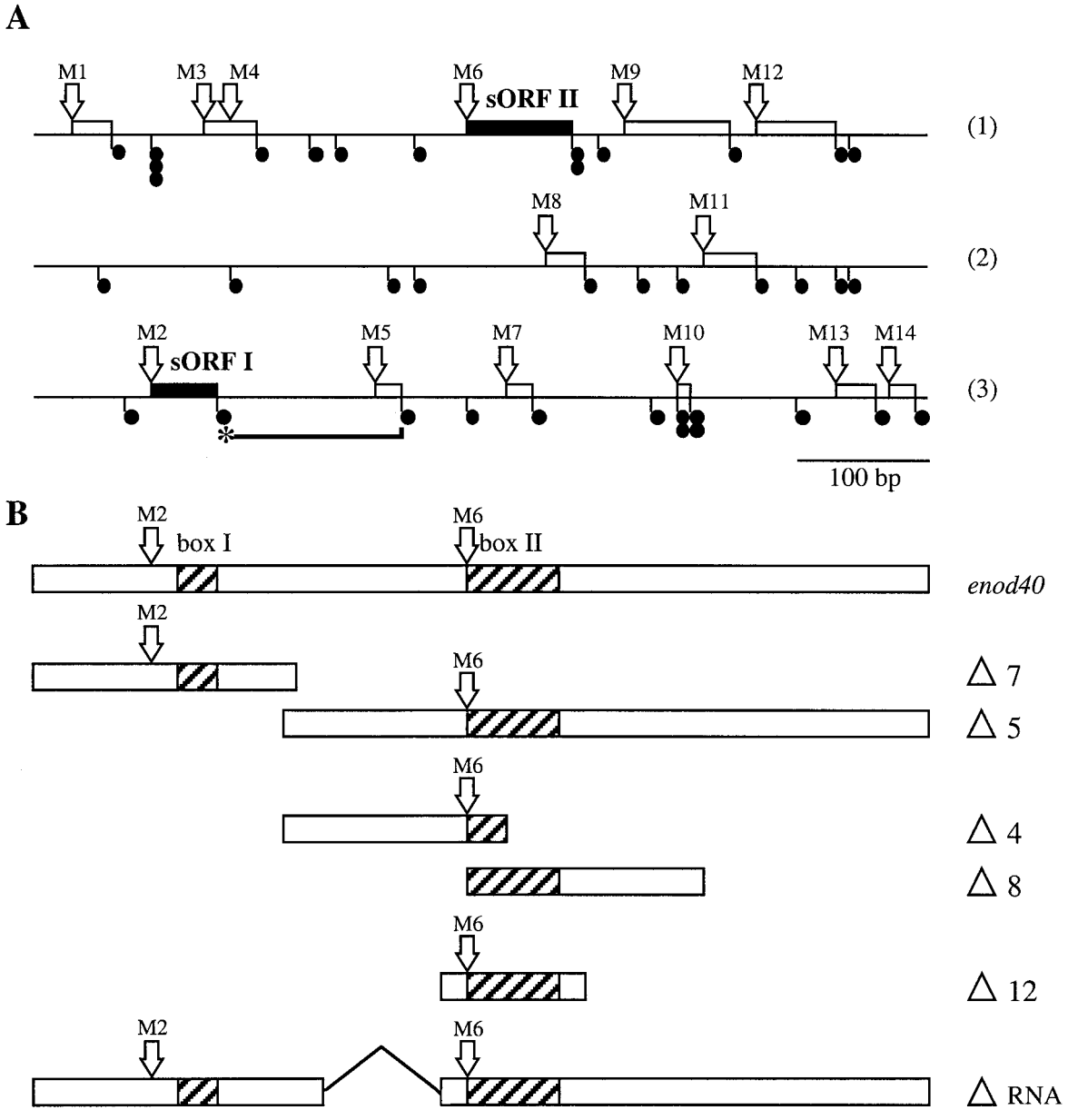

FIG. 1. Schematic representation of the *Mtenod40* cDNA sequence. (A) Each of the three possible reading frames is depicted separately (1 to 3). Open arrows marked M1 to M14 correspond to the different ATG codons (methionines) of the *Mtenod40* gene. Solid circles are stop codons (TAG, TAA, or TGA). ORFs are depicted as boxes, and the conserved sORF I and sORF II are marked. The complete *Mtenod40* transcript harboring the two conserved boxes and the two ATG codons of sORF I and II is shown. (B) Deletion series of *Mtenod40*. Boxes I and II as well as the ATG codons M2 and M6 are indicated for each deletion. For the ΔRNA construct, the region marked by a line was deleted. Note that M6 is absent from Δ8.

enod40 constructs into alfalfa roots. This technique uses gold microprojectiles to deliver soluble substances into cells within a very localized area (down to 150 μm) (34) and has previously been applied to study the effects of chitin oligosaccharides and Nod factors on nodule initiation (26, 36). We demonstrate here that two sORFs (I and II) as well as an inter-ORF region spanning a predicted RNA structure are involved in the regulation of *enod40* activity in *Medicago* roots. Using reporter gene fusions, translation of the two sORFs as well as the influence of the 5′ sORF I on translation of the 3′ sORF II was demonstrated, suggesting that this unusual nodulin gene may have a polycistronic nature. In vitro translation of purified *Mtenod40* transcripts containing point mutations allowed detection of a specific product starting from the initiation codon of the 5′ sORF I. These data indicate that sORF translation is required for *enod40* function in leguminous roots and suggest that sORF-encoded peptides may be important elements in regulatory mechanisms involving sORF-RNAs.

MATERIALS AND METHODS

Plant material and bacterial strains. Seedlings of *M. sativa* cultivar Sitel were germinated in water and grown aseptically. Inoculation with *Sinorhizobium me-*

liloti strain Rm41 for large-scale preparation of young nodule extracts in aeroponic tanks was performed as described earlier (12).

Escherichia coli CC118 [Δ(*ara-leu*) *araD* Δ*lacX74 galE galK phoA20 thi-1 rpsE rpoB argE*(Am) *recA1*] (20) and *E. coli* DH5α (*supE44 hsdR17 recA1 endA1 gyrA96 thi-1 relA1*) (17) were used for subcloning. *E. coli* XL1-Blue [*recA1 endA1 gyrA96 thi-1 hsdR17 supE44 relA1 lac* {F′ *proAB lacI*^{q}*ZΔM15 Tn*10 (Tet^r)}] (6) was used as the recipient of all plasmids with point mutations.

Construction of translational fusions of *enod40* sORFs and the *uidA* gene. A series of translational fusions to the *uidA* gene driven by the constitutive cauliflower mosaic virus 35S promoter were constructed. A vector (pDH51 5), containing the cauliflower mosaic virus (CaMV) 35S promoter fused to the reporter gene without the initiating methionine and instead having a polylinker, was used to clone different portions of the *Mtenod40* and *M. sativa enod40* (*Msenod40*) transcripts.

The constructs diagrammed in Fig. 2 were obtained by insertion of PCR products, using different *enod40* oligonucleotides, p*Mtenod40*/p*Msenod40* DNAs, and their derivatives as the template. In the case of plasmid M1GUS, an oligonucleotide (AATTCCAACTTCCCCACTACCTTTCTATGT) corresponding to the *Mtenod40* cDNA sequence up to and including part of the first sORF, was inserted in the vector. In order to find out whether the 3′ region might inhibit translation of sORF I, we introduced the 3′ region (Δ5; nucleotides 204 to 614 of the *Mtenod40* gene) immediately behind the *uidA* sequence in the in-frame translational fusion (pTra40M2, Fig. 2C). pTra40M2-Δ5 and pTra40M2-inv.Δ5 were prepared by subcloning Δ5 into pTra40M2 in the sense and antisense orientations, respectively (Fig. 2C). The sequences of all constructions were confirmed as mentioned below. Further details on plasmid construction are available upon request.

Construction of *enod40* mutants. All point mutations were introduced by the Quickchange site-directed mutagenesis kit (Stratagene), using synthetic oligonucleotide primers containing the desired mutation. For p*Mtenod40*-ACG sORF I, the primers were 5′-GTAATAAGGACGAAGCTTCTTTGTTGGG-3′ and 5′-CCCAACAAAGAAGCTTCGTCCTTATTAC-3′. For p*Mtenod40*-TCA sORF I (5.8 kDa), the primers were 5′-ATCCATGGTTCTTCAAACAAACATGGAG-3′ and 5′-CTCCATGTTTGTTTGAAGAACCATGGAT-3′. For p*Mtenod40*-mod.sORF I, the primers were 5′-GGGAAAAATCAATCCACGGCTCGTAAAACAAACATGG-3′ and 5′-CCATGTTTGTTTTACGAGCCGTGGATTGATTTTTCCC-3′. For p*Mtenod40*-ACG sORF II, the primers were 5′-GCTTTTGTTATAGCACGGCAAACCGGCAAGTC-3′ and 5′-GACTTGCCGGTTTGCCGTGCTATAACAAAAGC-3′. For p*Mtenod40*-TCA sORF I/TAG (3.8 kDa), the primers were 5′-CCTAAACAGTTAGCTTTGTGCTTTAGC-3′ and 5′-GCTAAAGCACAAAGCTAACTGTTTAGG-3′. (Underlined nucleotides indicate point mutations.)

Replacements were done in pBluescript pSK(+), and the sequences of the mutants were confirmed as described below.

p*Mtenod40*/p*Msenod40*-ACG sORF I and p*Mtenod40*-ACG sORF II are similar to p*Mtenod40* and p*Msenod40* but with a mutation in the ATG of sORF I and sORF II, respectively. p*Mtenod40*/p*Msenod40*-TCA sORF I and p*Mtenod40* mod.RNA are also similar to p*Mtenod40* and p*Msenod40*, but with a mutation in the stop codon of sORF I or modifications in the nucleotide sequence of sORF I (without changes to the encoded amino acid sequence), respectively. Plasmids p35S-*Mtenod40*/*Msenod40*, p35S-*Mtenod40*/*Msenod40*-ACG sORF I, p35S-*Mtenod40*-ACG sORF II, p35S-*Mtenod40*/*Msenod40*-TCA sORF I, and p35S-*Mtenod40* mod.RNA are similar to the plasmids described above but under control of the CaMV rRNA promoter.

Replacement of the *Mtenod40* sORF I sequence with the soybean *Glycine max Gmenod40* sORF I was done using primers 5′-GATCCTTGTTTGTAATAAGGATGGAGCTTTGTTGGCTCACAACCATC-3′ and 5′-CATGGATGGTTGTGAGCCAACAAAGCTCCATCCTTATTACAAACAAG-3′.

Primers were hybridized in vitro, and the double-stranded oligonucleotide was cloned in the *Bam*HI and *Nco*I sites of p*Mtenod40* to yield p*SoyMtenod40* carrying the 12-amino-acid-encoding sORF I of the soybean *Gmenod40* gene (31) followed by the complete 3′ region of *Mtenod40*. p35S-*SoyMtenod40* was constructed for expression of this RNA in plant cells (see above).

Construction of *enod40* deletions. For construction of the deletion series (Fig. 1B), we used plasmid pDH51 as the vector. These constructs were made by insertion of PCR products, using different *enod40* oligonucleotides and the p*Mtenod40* and p*Msenod40* DNAs and derivatives as the template. We obtained the following deletions: p35S-*Mtenod40*-Δ4 (nucleotides 204 to 350), p35S-*Mtenod40*-Δ6 (nucleotides 333 to 614), p35S-*Mtenod40*-Δ8 (nucleotides 333 to 460), and p35S-*Mtenod40*-Δ12 (nucleotides 310 to 460). p35S-*Mtenod40*-Δ5 (nucleotides 204 to 614) and p35S-*Mtenod40*-Δ7 (nucleotides 31 to 200) have been described previously (9). p*Mtenod40*-Δ5 and p*Mtenod40*-Δ7 are derived from pSK(+) and are similar to p35S-*Mtenod40*-Δ5 and p35S-*Mtenod40*-Δ7, respectively, but under control of the T3 promoter. The p35S-*Mtenod40*-Δ5-ACG sORF II and p35S-*Mtenod40*-Δ7-ACG sORF I are similar to p35S-*Mtenod40*-Δ5 and p35S-*Mtenod40*-Δ7, respectively, but with a mutation in the ATG of sORF II and sORF I, respectively. A series of constructions were carried out in which nucleotides 221 to 311 (corresponding to the RNA structure located between sORF I and sORF II) of the *Mtenod40* transcript were deleted. These constructions, p*Mtenod40*-ΔRNA and p*Msenod40*-ACG sORF I-ΔRNA, were introduced into pDH51, pSK(+), and the vector with the *uidA* gene. We used p*Msenod40* and derivatives as templates. The sequences of the deletions were confirmed as described below.

Nucleic acid techniques and in vitro translation assays. All steps in the cloning procedures were performed as recommended by the suppliers of the enzymes or as described before (33). Plasmids were analyzed by sequencing using a 373A automatic sequencer (Applied Biosystems) and the Pharmacia sequencing kit.

In vitro transcription of the p*Mtenod40* insert cloned in pSK(+) was performed with T3 polymerase under conditions for the generation of capped RNA using the Trans probe kit (Pharmacia). In vitro translation of purified transcripts was done using rabbit reticulocyte lysates and wheat germ extracts (Combination System; Promega) and either methionine or cysteine as the labeled amino acid. High-resolution sodium dodecyl sulfate-polyacrylamide gel electrophoresis (SDS-PAGE) of the in vitro translation products was performed as described below.

The constructs used for these experiments were described above with the exception of p*Msenod40*-TCA sORF I Δ3′ region, p*Msenod40*-TCA sORF I ΔpolyA, and p*Msenod40*-TCA sORF I/TGA. p*Msenod40*-TCA sORF I Δ3′ and p*Msenod40*-TCA sORF I ΔpolyA correspond to the p*Msenod40* gene but have a mutation in the stop codon of sORF I and lack either the 3′ region or the poly(A) tail of the gene, respectively. p*Msenod40*-TCA sORF I/TGA is similar to p*Msenod40* but contains a frameshift mutation in sORF I (*Nco*I digested and Klenow repaired), resulting in a translation product of 2.2 kDa.

The amount of *enod40* mRNA in mature nodules of *M. sativa* cv. Sitel was estimated on Northern blots using known amounts of in vitro-transcribed *Mtenod40* as the standard. Northern blotting using *Mtenod40* and *Msc27* probes was performed as described before (9).

Conventional particle gun bombardment. Particle bombardment using a Biolistic PDS-100/He particle gun (Bio-Rad) and β-glucuronidase (GUS) activity histochemical staining were performed as described before (9). *M. sativa* A2 suspension cells (5 days after subculture) were diluted to a cell density corresponding to a packed cell volume of 15% (vol/vol) and plated on Murashige-Skoog-based medium (Sigma M 5519; 3% [wt/vol] sucrose and 1% [wt/vol] Bacto-agar). Cells were grown overnight before bombardment.

Seedlings (5 days after germination) or plated cells from an alfalfa suspension culture were bombarded and stained for GUS activity 2 days later. At least 15 seedlings and three cell plates were bombarded per construct, and experiments were performed at least twice. GUS staining was done for at least 5 h at 37°C, and the number of blue spots was counted under a stereomicroscope. Vibratome (Micro-cut H1200; Bio-Rad) 80-μm sections were cut after embedding in 6% agarose.

Microtargeting. Microtargeting was performed using the setup described by Sautter et al. (34). Seedlings were plasmolysed by addition of 10% (wt/vol) sucrose and 3% (wt/vol) agar for 1 h prior to bombardment and transferred to Gibson medium 1 day after bombardment. Roots were bombarded in the area of emerging root hairs. A suspension of 1.4-μm gold particles was used at ca 0.5×10^6 particles/μl. DNA was used at a concentration of 1 μg/μl. Pressure was 100 bar, vacuum was −900 mb, and the size of restriction was 140 μm. Two days later, roots were cut and cleared by treatment with commercial bleach as described (9). Whole roots were analyzed under the light microscope (Polyvar; Reichert) for foci of dividing cortical cells by changing the focus to scan through the entire depth of the root. At least two separate experiments (testing a minimum of 15 plants) were performed for each construct. Embedding in paraffin and sectioning were performed as described (9).

Extraction and fractionation of peptides. Plant tissue was ground in liquid nitrogen and homogenized in extraction buffer (100 mM Tris-HCl [pH 8.0], 100 mM KCl, 10% [vol/vol] glycerol, 10 mM EDTA, 5 mM dithiothreitol, 1 mM phenylmethylsulfonyl fluoride). Homogenates were fractionated by centrifugation at $1,000 \times g$ for 10 min. The pellet was resuspended in Laemmli sample buffer for Western blots (Protocols and Applications Guide; Promega), and the supernatant was recentrifuged at $10,000 \times g$ for 10 min after the addition of 2% (vol/vol) Triton X-100. The resulting pellet was resuspended as above for Western blots, while the supernatant was used for both Western blots and enzyme-linked immunosorbent assay (ELISA).

High-resolution SDS-PAGE for the separation of peptides was performed as described (Protocols and Applications Guide; Promega), and blots were trans-

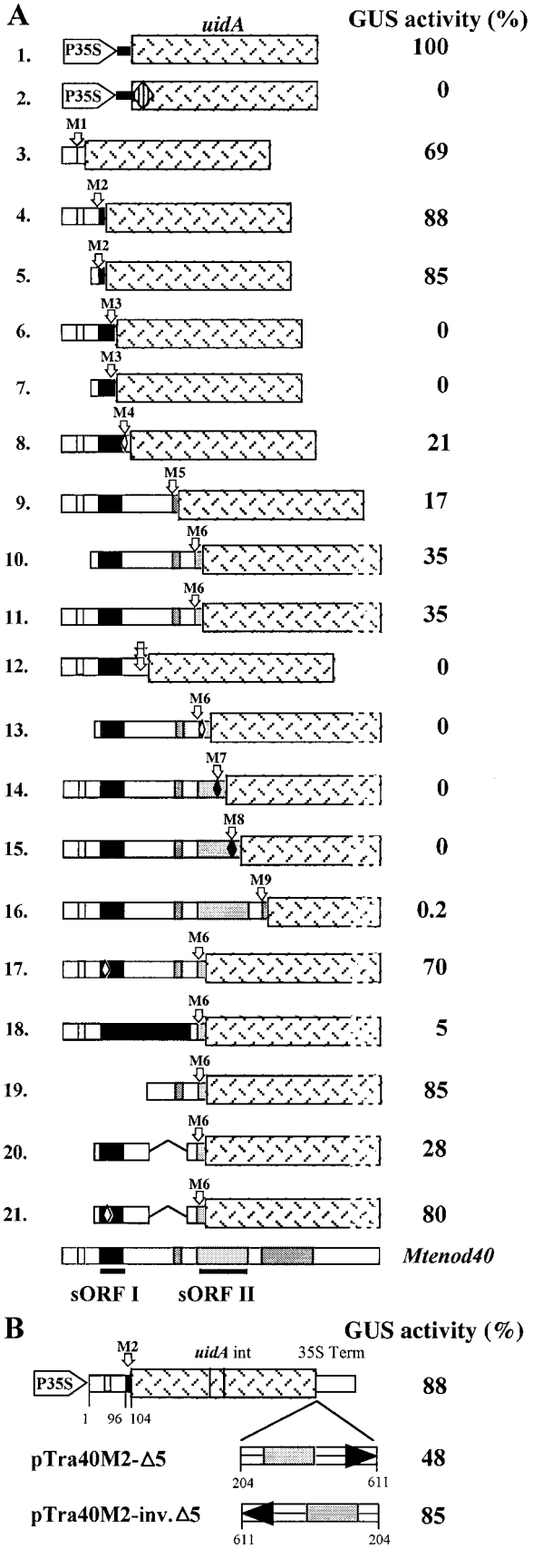

ferred onto 0.45-μm nitrocellulose membranes (Schleicher & Schuell) for Western analysis. High-pressure liquid chromatography (HPLC) for peptide detection was carried out using a reverse-phase column (Beckman Ultrasphere C_{18}; 2 by 150 mm; particle size, 5 μm) with a Beckman System Gold. Samples were eluted at 0.3 ml/min for 60 min with a linear 0 to 70% gradient (A, H_2O–0.05% trifluoroacetic acid [TFA]; B, 80% CH_3CN–0.05% trifluoroacetic acid). Eluted compounds were detected by their absorption at 214 nm.

Immunodetection of the MtENOD40 peptide. Polyclonal antibodies were produced in a rabbit by injection of synthetic sORF I peptide coupled to ovalbumin and affinity purified using the synthetic peptide and Affi-gel 10 (Bio-Rad) as described by the manufacturer. Secondary anti-rabbit immunoglobulin G antibodies coupled to alkaline phosphatase (Sigma) were used at a 1:2,000 dilution.

Western blot membranes were incubated for 1 h in blocking solution (5% dry milk in phosphate-buffered saline [pH 7.4]–0.1% Tween 20) before incubation overnight at 4°C in the primary anti-MtENOD40 antibody (diluted 1:200 in blocking solution). Incubation in the secondary antibody solution was for 2 h at 4°C. Signals were detected using 5-bromo-4-chloro-3-indolylphosphate–nitroblue tetrazolium (Sigma). For the supernatant fraction, 70 μg of total protein was loaded per lane.

For ELISA, the synthetic MtENOD40 peptide, nodule protein supernatants, or a combination of the two were fixed onto ELISA plates and incubated with the primary antibody at a dilution of 1:1,000 for 30 min at room temperature. Incubation with the secondary antibody was performed for 2 h at room temperature. Fluorometric detection of the signal was performed using 1 mg of *para*-nitrophenyl phosphate (Sigma) per ml. Up to 600 μg of total protein was loaded per microtiter well. Immunocompetition assays were done by fixing 10 ng of the MtENOD40 synthetic peptide on an ELISA plate and incubating with anti-sORF I antibodies overnight in the presence of purified peptide or soluble extracts of roots or nodules. After washing and incubation with the secondary antibody, detection of the signal was done as above.

Sequence analysis. The genomic *enod40* sequence was analyzed using GCG programs (University of Wisconsin, Madison) to estimate the percentage of GC. For prediction of the RNA secondary structure, we used the method described before (12), but analyzing window sizes of 30 to 301 nucleotides and scanning with a increment path of 2 bp for each calculation of the number of standard deviations ($n\sigma$) at different gene positions.

FIG. 2. Reporter gene activity induced by *Mtenod40* derivatives, with different ATG codons (methionines) fused in frame to the *uidA* coding sequence. Translational activity was measured after particle gun bombardment of the DNA constructs into seedlings. The activity values are the means of three to five independent experiments and were calculated relative to the expression value for the positive control (P_{35S}-*uidA*; with its own ATG, 100%). The relative expression level of a given construct varied within a maximum of 20% of the indicated value between different experiments.(e.g., for AUG6, 35% ± 7%; for AUG5, 17% ± 4%). (A) The striped diamond in the p35S*uidA* construct indicates a polylinker replacing the initiating ATG codon (methionine) of the *uidA* coding sequence. This vector was used to clone the different *Mtenod40* regions up to the indicated ATG codon (M1 to M9). Arrows marked M1 to M9 correspond to the different ATG codons (methionines) of the *Mtenod40* gene that were fused to *uidA*. The triple arrow (construct 12) indicates fusions in the three reading frames after sORF I to test whether its stop codon arrests translation. Solid boxes indicate selected sORFs present in the *Mtenod40* gene. The open diamonds indicate a point mutation in the ATG start codon of sORF I or sORF II (M2 or M6; changing ATG to ACG) or the internal ATG codon (methionine) of M3 sORF (M4), and the solid diamonds show ATG codons of sORFs in other frames (M7 and M8). Deletions in the *Mtenod40* gene are indicated as lines. Note that M4 is internal to the M3 sORF but lies 8 bp after the stop codon of sORF I. The M4 sORF codes for a 7-amino-acid peptide. (B) Constructs used to test the influence of the 3′ region (Δ5) on translation of sORF I. This sequence was inserted in the 5′-to-3′ (pTra40M2-Δ5) and 3′-to-5′ (pTra40M2-inv.Δ5) direction, downstream of the *uidA* sequence. int, intron; 35S Term, 35S terminator [poly(A) signal].

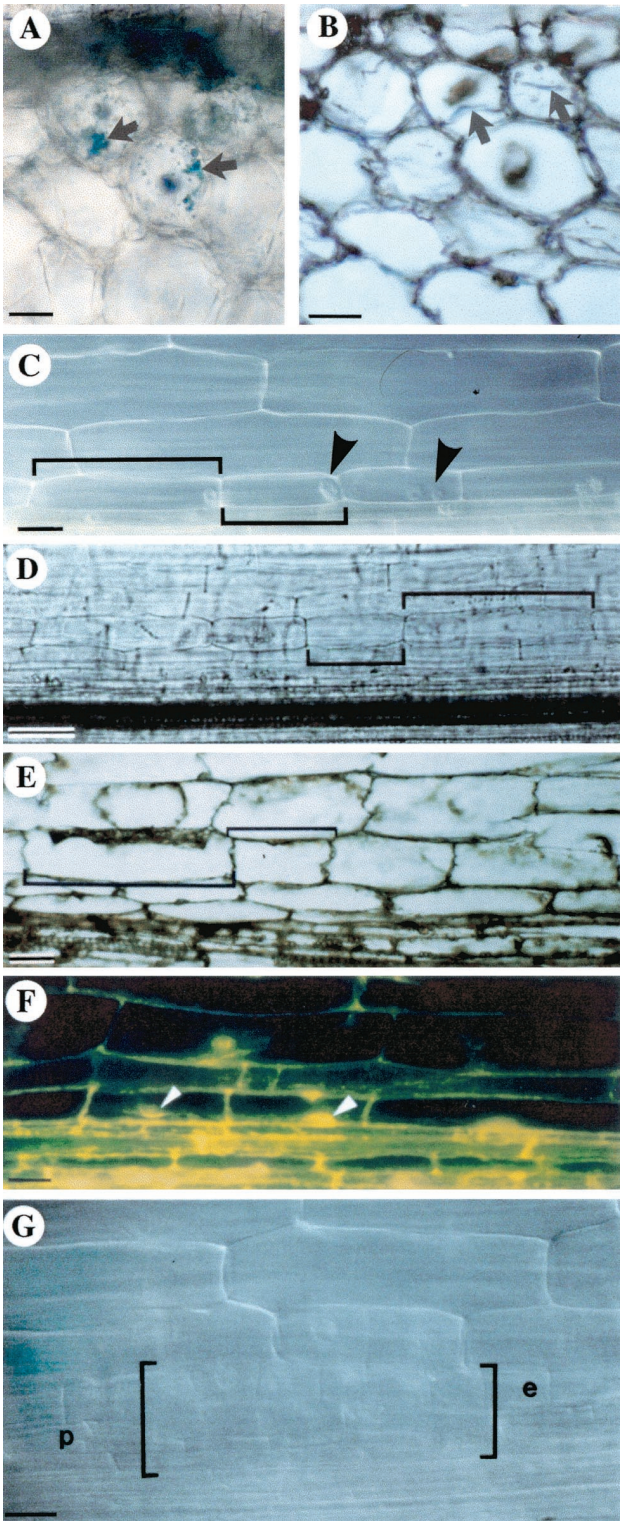

FIG. 3. Microscopic analysis of alfalfa roots fixed 2 days after microtargeting with *enod40* derivatives. (A and B) Transversal sections showing transient expression of an *Mtenod40-uidA* translational fusion in outer cortical cells of alfalfa roots. The colored GUS reaction product is indicated by arrows: (A) 80-μm section; (B) 8-μm section. (C to F) Cortical cell divisions 2 days after microtargeting. Note the difference in cell length of recently divided and nondivided cells (brackets). Nuclei are indicated by arrowheads. (C and D) Whole roots in phase contrast, showing cortical cell divisions. (E and F) Sections (8 μm) of cortical cell divisions as seen in bright-field mode (E) and fluorescence (F). (G) Early root primordium. Extensive concomitant divisions (within brackets) are found in the pericycle (p) and endodermis (e). Bars: 25 μm (A, E, and F), 15 μm (B), 20 μm (C and G), and 50 μm (D).

RESULTS

Analysis of *Mtenod40* sORF translation in alfalfa roots. The *Mtenod40* transcript is approximately 700 bp long and contains several sORFs in all three reading frames (Fig. 1A). One of these, sORF I, is highly conserved and corresponds to peptides of 10 to 13 amino acids in different species (42). The *Mtenod40* transcript contains the longest 5′ region upstream of nucleotide box I published so far (12), as demonstrated by reverse transcription-PCR (data not shown). To investigate the translational capacity of *Mtenod40*, a series of translational fusions to the *uidA* gene driven by the constitutive cauliflower mosaic virus 35S promoter were constructed using a vector without an initiating methionine and having instead a polylinker. In this way, the different AUG codons present in the *Mtenod40* sequence could be assayed for their capacity to initiate translation. After conventional particle gun bombardment, the constructs were transiently expressed in alfalfa seedlings. Two days later, GUS activity, converting X-D-glucuronic acid (X-D-GlcA) into a blue insoluble product, was estimated as the number of blue spots on roots compared to a 35S-*uidA* control (Fig. 2). The relative values given in Fig. 2 reflect the observed number of blue cells (in which GUS activity reached the threshold level required for detecting a blue spot on the root), related to the number of cells obtained when the same amount of 35S-*uidA* control DNA was bombarded (35S-*uidA*, 100%; Fig. 2A, construct 1). The vector used had no activity itself (Fig. 2A, construct 2). In addition, bombarding a translational fusion of the *Mtenod40* promoter and *uidA* also yielded GUS activity in alfalfa cells, although at reduced levels compared to the 35S CaMV promoter fusion (data not shown).

The fusion with the start codon of the 13-amino-acid oligopeptide (sORF I) sequence of *Mtenod40* in frame with the *uidA* gene (nucleotide 103 of *Mtenod40*; pTra40-M2) was efficiently translated (Fig. 2A, construct 4) despite the presence of a preceding 8-amino-acid sORF. Translation was observed in epidermal and outer cortical cells of intact roots (Fig. 3A and B) as well as in cultured cells (data not shown). In contrast, translation of *uidA* was abolished when the reporter gene was fused to a second out-of-frame ATG located within the 13-amino-acid sequence (nucleotide 130 of *Mtenod40*; pTra40-M3; Fig. 2A, constructs 6 and 7). Thus, the AUG of sORF I is recognized as an efficient translation start site, in contrast to the internal AUG codon, which is present in another frame. Furthermore, translation of the preceding 8-amino-acid sORF was also very efficient, suggesting that sORFs do not prevent reinitiation at the following ORF (Fig. 2A, construct 3). Deletion of the first sORF did not affect translation of sORF I.

Then, the reporter gene was fused to the next AUG codon, M4, which is located 8 bp after the stop codon of sORF I within the M3 sORF (Fig. 1A) and codes for a 7-amino-acid peptide. Translation was detectable, albeit inefficient (Fig. 2A, construct 8). The next ATG, M5, the start of a 5-amino-acid

sORF, also showed reduced translation, whereas M6, corresponding to the sORF-spanning region 2 (sORF II), was clearly translated (35%; Fig. 2A, constructs 9 to 11). To confirm that the stop codon of sORF I arrested protein translation, fusions downstream in the three reading frames were constructed. Translation was not detected in any case (Fig. 2A, construct 12). Fusions to AUG codons of other reading frames within sORF II (M7 and M8) or after sORF II (e.g., M9) also exhibited undetectable or very low levels (less than 1%) of translation (Fig. 2A, constructs 14 to 16).

Mutation of ATG codon M6 completely abolished GUS activity, indicating that sORF II translation started from this codon (Fig. 2A, construct 13). Interestingly, even between two *Medicago* species (*M. sativa* and *M. truncatula*), sORF II is not conserved in either size or amino acid sequence except for the amino acids encoded in the region of the so-called box II (Fig. 1). Moreover, AUG M6 only exists in *enod40* genes of a few legume species and tobacco, and the nucleotide sequences of the different *enod40* genes after box II are not conserved.

These results suggest that sORFs do not arrest 5′-to-3′ ribosome scanning and that reinitiation can occur along the *enod40* transcript. Two sORFs spanning the conserved nucleotide regions of *Mtenod40* can be efficiently translated in root tissues.

Activity of the different *Mtenod40* regions depends on translation of sORFs. Expression of *enod40* in roots resulted in cortical cell divisions (9). In order to study the molecular mechanism of *enod40* action, a microtargeting apparatus was used to introduce DNA in alfalfa root cells to monitor events related to *enod40* expression in a defined root region. Two days after microtargeting, the bombarded area was inspected for cortical cell division. Particles were found only in superficial cell layers (epidermis and outermost cortex) and were used to localize the bombarded area (diameter, less than 0.5 mm). Cell divisions detected in the inner cortex below this area (Fig. 3), without divisions in the underlying pericycle and endodermis, were observed as either (i) foci of recently divided cells showing a dense cytoplasm and conspicuous nuclei (Fig. 3C) or (ii) foci of divided cells that had already started to elongate (Fig. 3D). Sectioning confirmed the presence of divided cells (Fig. 3E and F). Early root primordia (Fig. 3G) were distinguished from cortical cell divisions by the occurrence of concomitant, extensive divisions of the pericycle, i.e., below the endodermis, which is recognized by the presence of Casparian strips and a strong autofluorescence.

The *enod40* activity of different constructs was monitored in a semiquantitative manner by counting the number of foci of dividing cortical cells. Transient expression of the *Mtenod40* construct in alfalfa roots induced cortical cell divisions at high frequency, giving an f_{div} value (cell division foci per root) of 0.51. This frequency is more than two times higher than those obtained in our previous experiments using conventional particle bombardment of whole roots from transgenic alfalfa plants carrying an *Msenod12A* promoter-*uidA* fusion (9). The empty vector had no effect (f_{div} = 0.02; Table 1). In agreement with our previous experiments, constructs spanning either box I or II had similar activity (corresponding to Δ7 and Δ5, respectively; Fig. 1B), as both also induced divisions at high frequency (Table 1). Mutating the start codon of the 13-amino-acid peptide sequence (ATG changed to ACG; p35S-Δ7-ACG sORF I) abolished the cell division-inducing activity of Δ7 (f_{div} = 0.03), suggesting that translation of sORF I is required for activity. Mutating the ATG codon of sORF II yielded a Δ5 derivative with highly reduced activity. Deletions containing the conserved nucleotide box II but not the entire sORF II did not show significant activity (Table 1, p35S-*Mtenod40*-Δ8 and p35S-*Mtenod40*-Δ4, respectively). In contrast, a short region spanning the unmodified sORF II retained biological activity, indicating that translation of this sORF might be responsible for the induction of cortical cell divisions elicited by Δ5 (Table 1, p35S-*Mtenod40*-Δ12). These values are significantly different, as demonstrated by a chi-square statistical test ($P < 0.01$).

TABLE 1. Microtargeting of alfalfa seedlings with *enod40* DNA constructs

Construct	No. of foci[a]	No. of roots examined	f_{div} ± SE[b]
pDH51	1	64	0.02 ± 0.02
p35S-*Mtenod40*	18	35	0.51 ± 0.09
p35S-*Mtenod40*-Δ7	8	20	0.40 ± 0.11
p35S-*Mtenod40*-Δ5	11	30	0.37 ± 0.09
p35S-*Mtenod40*-Δ7-ACG sORF I	1	38	0.03 ± 0.03
p35S-*Mtenod40*-Δ5-ACG sORF II	1	15	0.07 ± 0.07
p35S-*Mtenod40*-Δ4	3	20	0.15 ± 0.08
p35S-*Mtenod40*-Δ8	0	20	0.00 ± 0.00
p35S-*Mtenod40*-Δ12	6	12	0.50 ± 0.15
p35S-*Mtenod40*-ACG sORF I	4	46	0.09 ± 0.04
p35S-*Msenod40*-ACG sORF I	1	9	0.11 ± 0.11
p35S-*Mtenod40*-TCA sORF I	2	33	0.06 ± 0.04
p35S-*Mtenod40*-mod.sORF I	8	27	0.30 ± 0.09
p35S-*SoyMtenod40*	1	15	0.07 ± 0.07
p35S-*Mtenod40*-ACG sORF II	2	15	0.13 ± 0.09
p35S-*Mtenod40*-ΔRNA	2	15	0.13 ± 0.09

[a] Number of cortical cell division foci observed 2 days after microtargeting.
[b] Number of cortical cell division foci per bombarded root.

Thus, microtargeting of *Mtenod40* and two nonoverlapping deleted derivatives induced a cell-specific growth response in alfalfa roots. The cortical cell division-inducing activity observed for *enod40* deletions required the translation of two sORFs of 13 and 27 amino acids, sORFs I and II, respectively, spanning the conserved nucleotide boxes of the *enod40* transcript.

Translation of sORF I and sORF II regulates *Mtenod40* activity in alfalfa roots. Neither in Northern blots nor in cDNA libraries have we identified *Mtenod40* cDNAs corresponding only to Δ7 or Δ5 (not shown). Therefore, we decided to study the effects of sORF translation on the complete *Mtenod40* transcript. Microtargeting of the *Mtenod40* sequence with a mutated start codon for sORF I (p35S-*Mtenod40*-ACG sORF I and p35S-*Msenod40*-ACG sORF I; Table 1) had significantly reduced activity (f_{div} = 0.09 and 0.11, respectively). This was surprising, since the activity of the 3′ region of *Mtenod40* (see above) was expected to be retained in this derivative (only lacking sORF I). In addition, a construct in which the stop codon of the 13-amino-acid peptide-encoding sequence was mutated (p35S-*Mtenod40*-TCA sORF I), resulting in a longer sORF incorporating extra codons (up to 59 amino acids; as-

terisk in Fig. 1A), was also inactive (Table 1; $f_{div} = 0.06$). The nucleotide changes assayed might disturb either translation of the peptide or the mRNA in this region.

To confirm that sORF I was responsible for activity, a mutant *Mtenod40* sequence was created in which the 13-amino-acid peptide-encoding nucleotide sequence was modified while keeping the amino acid sequence intact (taking advantage of codon degeneracy). This yielded a construct (p35S-*Mtenod40*-mod.sORF I) with significantly high activity ($f_{div} = 0.30$), confirming that the translation product of the 13-amino-acid sORF is crucial for *enod40* activity. Finally, the *Mtenod40* sORF I sequence was replaced by a 12-amino-acid-encoding sequence corresponding to the soybean *Gmenod40* sORF I peptide (33). This p35S-*SoyMtenod40* derivative was inactive (Table 1; $f_{div} = 0.07$). This confirmed that the sORF I-derived peptide is essential for *Mtenod40* activity.

These experiments also suggest that translation of sORF II may require translation of sORF I. To test this hypothesis, we assayed constructs in which *uidA* was fused to the ATG-M6 of sORF II with either a mutated ATG or TAA codon in sORF I (Fig. 2A, constructs 17 to 19; cf. construct 11). Mutating the initiating codon of sORF I increased the translational activity of sORF II, whereas increasing the size of sORF I dramatically reduced the capacity to reinitiate translation at sORF II. Hence, the level of sORF II translation does not correlate with the biological activity of the mutated *Mtenod40* transcripts. Nonetheless, a point mutation of the ATG of sORF II abolishing its translation (Fig. 2A, construct 13) reduced the biological activity of *Mtenod40* (Table 1; $f_{div} = 0.13$). This indicates that translation of sORF II is important for cell division activity of the *Mtenod40* transcript.

From these experiments, we concluded that translation of both sORF I and sORF II is required for full *Mtenod40* activity. The effect of the 3′ *Mtenod40* region in alfalfa roots depends on the presence and correct size and sequence of the 13-amino-acid peptide encoded by sORF I, even though deletions spanning either sORF I or sORF II are active. These results revealed a complex level of regulation acting on the *Mtenod40* mRNA and are in line with the fact that nucleotide boxes I and II are highly conserved in *enod40* genes from several species.

***enod40* sORF-encoded oligopeptides require a minimum size to be detected by in vitro translation.** Having shown that the start codon of the *Mtenod40* 13-amino-acid sORF I can be recognized as a translation start site (in bombarded roots) and that sORF I is required for *enod40* activity, we searched for the presence of the encoded peptide in planta by several methods based on immunodetection. Polyclonal antibodies against the 13-amino-acid MtENOD40 peptide coupled to ovalbumin were prepared and affinity purified using the synthetic peptide. In Western blots using high-resolution gels optimized for detection of small peptides, these antibodies specifically recognized as little as 20 ng of the synthetic MtENOD40 13-amino-acid peptide, giving a band at 1.5 kDa (Fig. 4A), whereas the preimmune serum did not react with this sample. In ELISA, as little as 1 ng of synthetic peptide could be detected (data not shown). Then, we assayed total extracts and subcellular fractions of roots and mature nodules using both Western blots (70 μg of total protein was loaded per lane) and ELISA (up to 600 μg of total protein was loaded per microtiter well). Moreover, ELISA was also used to test fractions obtained by separating up to 600 μg of protein extract from mature nodules through HPLC. Similarly, several subcellular fractions of root extracts (corresponding to soluble, nuclear, and microsomal fractions) were tested at different time points after inoculation of *M. sativa* with *S. meliloti*. Even though weak signals could be detected at higher molecular weights, no signal corresponding to a small oligopeptide was detected either during early nodule development or in mature nodules by any method using the different extraction procedures (data not shown). However, immunocompetition experiments revealed the presence of small amounts of an antigen related to the 13-amino-acid peptide in nodules (Fig. 4B). Interestingly, quantification of *enod40* transcripts by Northern blotting indicated that they constitute approximately 0.5% of the total amount of mRNA in the nodule, accumulating rapidly during early nodule development (Fig. 4C).

Thus, while *enod40* is a very abundant mRNA in the nodule, the oligopeptide is either present at a very low concentration or unstable under our extraction conditions. To test the latter possibility, we added up to 2 μg of the synthetic peptide to nodule extracts, and the presence of the peptide was tested at different time points by Western blotting. The immunological signal had already disappeared after 1 min of incubation (Fig. 4E). Nevertheless, the peptide was stable in a soluble fraction inactivated by SDS treatment or fractionated to retain constituents of less than 10 kDa (Fig. 4E). These data indicate that oligopeptides may be highly unstable in plant extracts, due either to degradation or to binding to a component that masks it very rapidly from the antibodies.

We then tested the in vitro translation of various amounts of purified *Mtenod40* RNA (transcribed in vitro) using both wheat germ and reticulocyte extracts (Fig. 5). No significant signal was observed in several experiments (Fig. 5A, constructs 1 and 2) using either *Msenod40* or *Mtenod40* RNAs. The occasionally translated short peptides (such as those depicted in Fig. 5B, lane 2) showed no correlation with the synthesized peptide using HPLC or immunoprecipitation (data not shown; see below). In addition, no in vitro translation products were observed using deletion derivatives of *enod40* (Fig. 5, constructs 9 and 10). We tested the stability of the putative oligopeptide encoded by sORF I by adding the synthetic 13-amino-acid peptide to the extracts used for in vitro translation. The immunological signal disappeared again very rapidly (less than 1 min) (Fig. 4F). It is likely that the short unstable *enod40* peptides need to be coupled to or protected by a large protein or subcellular structure to avoid rapid degradation. An *enod40* derivative containing a point mutation in the stop codon of sORF I that should give translation of a 59-amino-acid peptide was then tested (Fig. 1A, asterisk). A clear band of the expected size was observed on gels after in vitro translation (Fig. 5, constructs 3 and 5). This in vitro translation product was not detected when the start codon of sORF I was mutated (Fig. 5, construct 4), further confirming that it corresponds to the mutated sORF I. Moreover, constructs with point mutations encoding the predicted peptides of 39 and 22 amino acids, respectively (Fig. 5, constructs 6 and 7), were tested. These transcripts are almost identical to *Mtenod40*, suggesting that the ATG of sORF I is indeed recognized but that peptides of less than 39 amino acids are very unstable and therefore can-

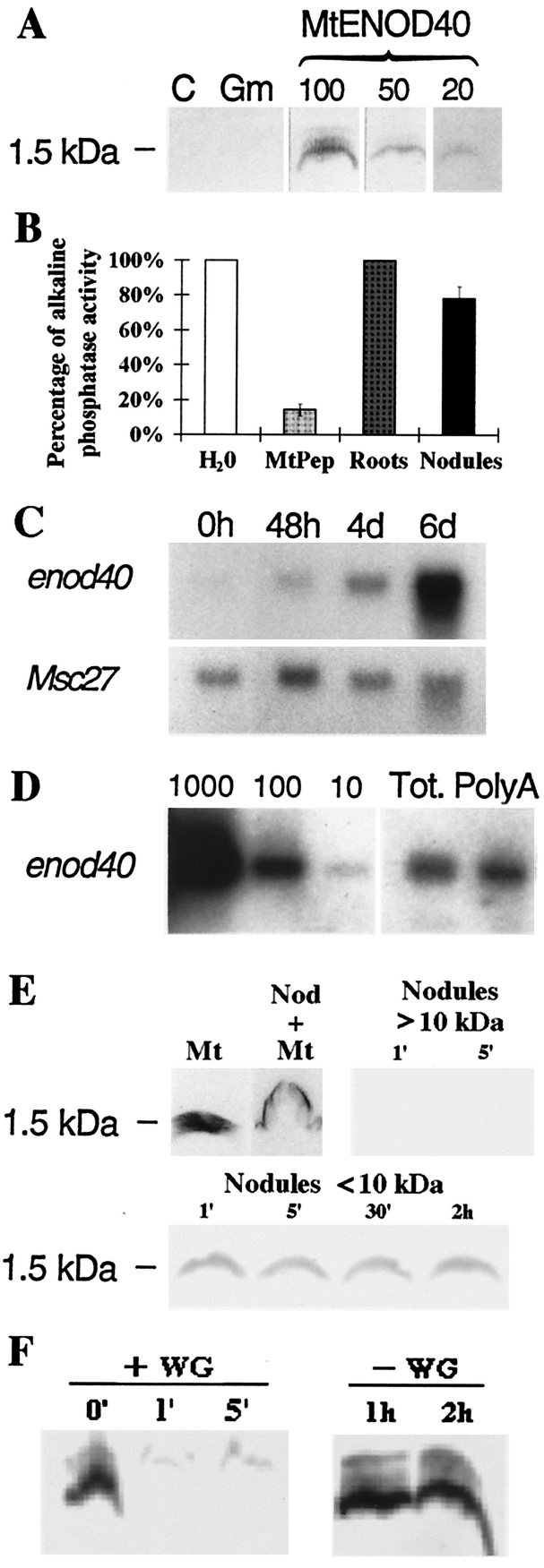

not be detected under conditions for in vitro translation. This also suggests a correlation between the minimum size of a sORF whose product can be detected by in vitro translation and, as mentioned in the previous section, the maximum size of an upstream sORF that allows further 3′ translation (Fig. 2A, construct 19). As expected, small peptides could not be detected using p*Mtenod40*-modified sORF I or p*Mtenod40*-ACG sORF I (Fig. 5, constructs 12 and 13). The latter one occasionally showed short translated peptides similar to p*Mtenod40*, confirming that these are not sORF I related. Finally, the presence of a poly(A) tail in the *enod40* mRNA was required for detection of the in vitro translation products (Fig. 5, construct 11).

To explain the presence of two biologically active regions in the *enod40* transcript, it was previously hypothesized that the 3′ region might inhibit translation of sORF I (42). We tested this hypothesis by two different approaches. First, we introduced the 3′ region (Δ5) immediately downstream of the *uidA* sequence in the in-frame translational fusion with sORF I (pTra40M2-Δ5). Translation was reduced by half compared to pTra40M2 (Fig. 2B). Introducing this 3′ sequence in an inverted position (pTra40M2-inv.Δ5) yielded translation at the same level as that obtained without it. Second, in vitro translation of the 59-amino-acid sORF I *Mtenod40* derivative (with a mutated stop codon) in the presence or absence of the 3′ *Mtenod40* Δ5 sequence (Fig. 5, constructs 3 and 8) showed no significant effect of this 3′ region on sORF I translation.

Thus, the ATG codon of sORF I is recognized as a translation start site in roots and during in vitro translation. Detection of peptide products corresponding to an encoded sORF by in vitro translation requires a minimum size. The MtENOD40 oligopeptide(s) might be very difficult to detect due to high instability, even in plant tissues where transcripts accumulate abundantly. Nevertheless, epitopes related to the sORF I-en-

FIG. 4. Analysis of *enod40* gene products and their stability. (A) Western blot of synthesized peptides showing the specificity of anti-ENOD40 13-amino-acid peptide antibodies. Lane C, 100 ng of a control peptide with a rearranged 13-amino-acid sequence; lane Gm, 100 ng of the *Gmenod40* 12-amino-acid peptide (31); lanes MtENOD40, 100, 50, or 20 ng of the *Mtenod40* 13-amino-acid peptide as marked. (B) ELISA immunocompetition assays. Root and nodule soluble extracts were used against 10 ng of bound *Mtenod40* peptide. Antibodies were added alone (water control) in the presence of 500 ng of synthetic peptide (MtPep) or 500 μg of root or nodule extract. (C) Northern blot showing hybridization of an *Mtenod40* probe to RNA isolated from *S. meliloti*-inoculated alfalfa roots during nodule development. Time after inoculation is indicated (hours or days [d]). The constitutively expressed *Msc27* was used as a control for RNA loading. (D) Northern quantification of the *Mtenod40* transcript amount in nodules. Lane Tot, 5 μg of total nodule RNA (approximately 2% corresponds to mRNA); lane PolyA, 200 ng of nodule poly(A)-containing RNA; 1,000, 100, and 10 pg of in vitro-transcribed *Mtenod40* mRNA were used for calibration. Quantification of the hybridization signals indicates that *Mtenod40* signals correspond to 50 and 80 pg for total and poly(A) RNA, respectively. (E and F) Western blots showing MtENOD40 13-amino-acid peptide stability in nodule extracts (E) and in wheat germ in vitro translation extracts (F). Mt, MtENOD40 peptide without extract; Nod+Mt, nodule extract denatured with 1% SDS before adding the peptide; nodule fractions enriched in proteins of >10 or <10 kDa incubated with the peptides for the indicated time periods (minutes). +WG and −WG, with and without wheat germ extracts for the indicated time periods (minutes or hours), respectively.

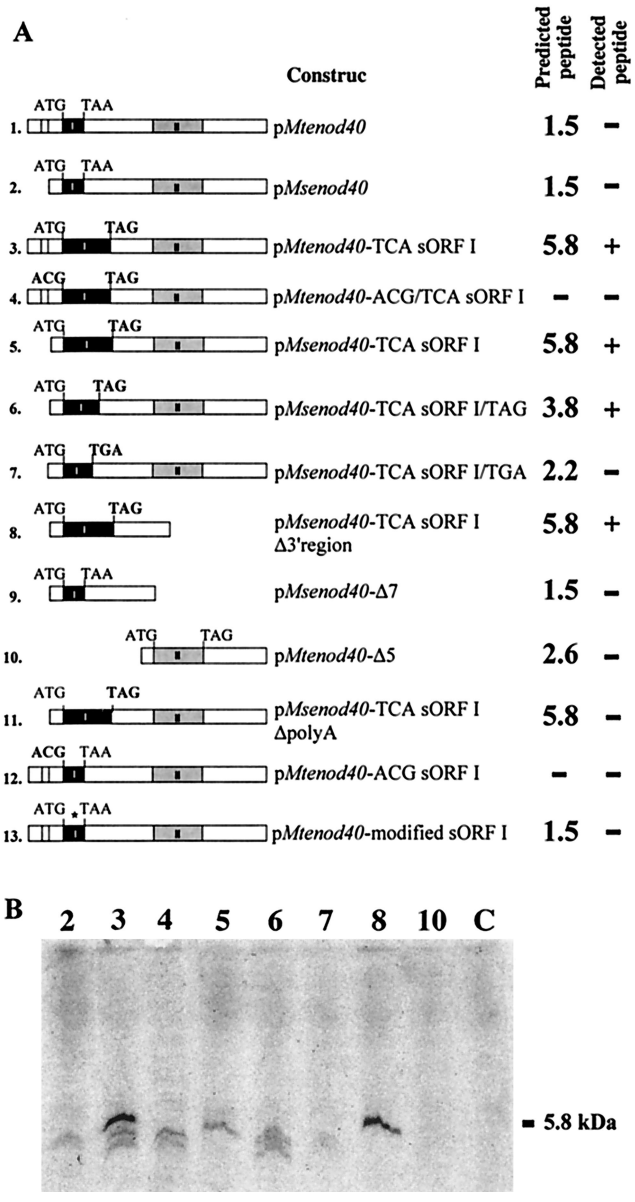

FIG. 5. In vitro translation of *Mtenod40* and *Msenod40* RNA using wheat germ extracts. (A) Predicted peptides after in vitro translation of different *Mtenod40* mRNA derivatives. Detection of an in vitro translation product of the expected size is denoted by +. Solid boxes indicate sORF I and sORF II present in the *Mtenod40* and *Msenod40* genes. TAG and TGA in bold type indicate the stop codon for a modified sORF I peptide after creation of a point mutation in the stop codon for sORF I (TAA to TCA). ACG in bold type indicates a point mutation changing the ATG start codon of sORF I to ACG. Predicted peptide values are in kilodaltons. (B) Radioactive products detected after in vitro translation of the different *enod40* constructs, numbered as in panel A. Lane C, control translation reaction without mRNA.

coded peptide may exist in nodule extracts. The 3′ *enod40* region did not show any significant effect per se on translation of the 5′ sORF I.

Deletion of an *Mtenod40* inter-sORF region spanning a predicted RNA structure affects biological activity. Translation of *Mtenod40* sORFs is necessary for full biological activity, although translation of either sORF is sufficient in the deletion-containing mRNAs. Hence, our results suggest that a novel type of regulation of sORF activity may exist in the whole transcript that is lacking in the deletion derivatives. We therefore decided to analyze the *Mtenod40* mRNA in a genomic context. The sequence of a 3-kb *Mtenod40* genomic region (containing a 1-kb upstream and a 1.3-kb downstream region) was determined, and its GC percentage was analyzed. The *Mtenod40* mRNA separates from the isochore of the *Medicago* genome (38% GC 4) from the beginning of the transcript (Fig. 6B), suggesting a larger functional *Mtenod40* region than that corresponding to the sORFs. In our previous work, we proposed that the *Mtenod40* transcript codes for a highly structured RNA, based on calculations of the free energy of folding (12). By applying the same computer program using small (around 40 bp) scanning windows, we could now predict the presence of a highly structured RNA region which is located between the two sORFs of the *Mtenod40* transcript (Fig. 6C, first panel; $n\sigma > 5$; this number illustrates that this structure has a very low probability of appearing randomly on the same nucleotide sequence; for details see reference 12). This structure lies on the functional *enod40* region predicted by the isochore analysis of the nucleotide sequence to lie between the two conserved nucleotide boxes. Therefore, a deletion was made to modify this "inter-sORF" region (Fig. 1, ΔRNA) without affecting the coding sequences of the sORFs. This *Mtenod40* derivative showed a significant reduction in biological activity (Table 1, $f_{div} = 0.13$) after microtargeting, indicating that the RNA region between sORF I and sORF II is also required for gene function. To show whether an RNA structure may be conserved, the presence of RNA structures was sought in various *enod40* genes (Fig. 6C, panels 2 to 4). Interestingly, in a relatively homologous position (between the two conserved nucleotide boxes), highly probable predicted structures were found in *enod40* genes from white clover, soybean, and rice (see Discussion).

We then tested whether this deletion of the inter-ORF region of the *Mtenod40* transcript would inactivate translation of the sORFs. A translational fusion to sORF II in which this RNA region was deleted was used to bombard roots. No effect on translation of sORF II was detected in comparison to the fusion containing this RNA region (Fig. 2B, construct 20) (cf. construct 11). To analyze the effect of this region on sORF I translation, we introduced a point mutation in the sORF I ATG in a corresponding construct. Inactivation of sORF I affected sORF II translation as reported for the complete *enod40* transcript (Fig. 2B, construct 21; cf. construct 17), indicating that sORF I is likely translated.

Therefore, an RNA region present between the *Mtenod40* sORFs regulates the elicitation of cortical cell division, most likely without perturbing translation of the sORFs. These results reveal a new level of regulation acting on *enod40* activity.

DISCUSSION

Peptides encoded in sORFs may act as signals during the induction of cortical cell divisions in roots. Here we demonstrated that *enod40*-induced cell division in the alfalfa root inner cortex depends on the translation of two sORFs. Our assay was based on the introduction of *Mtenod40* by microtargeting in the region of emerging root hairs where rhizobia and

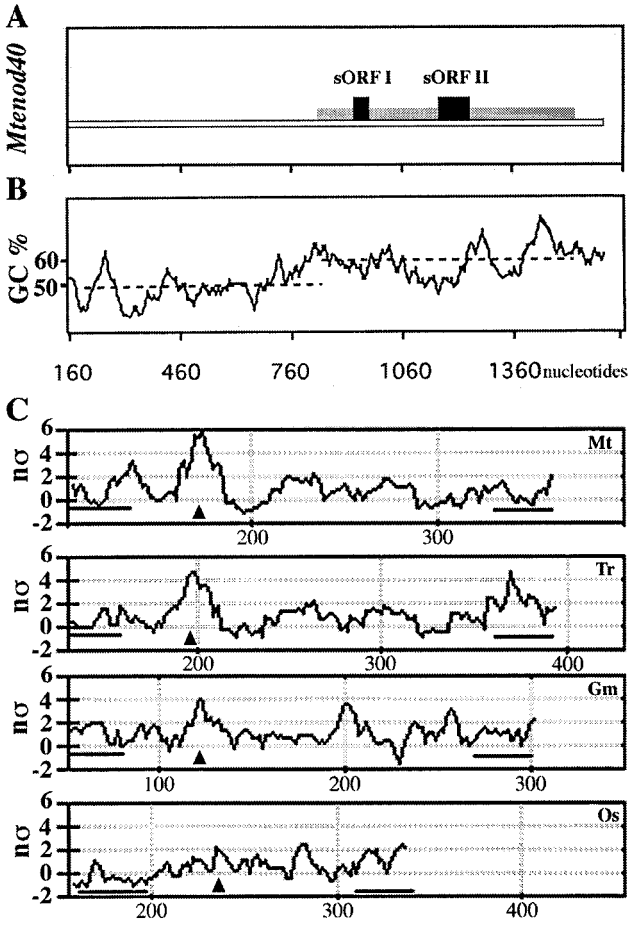

FIG. 6. Structural analysis of the *Mtenod40* sequence. (A) Schematic representation of the *Mtenod40* genomic sequence (accession number X80263). The cDNA sequence is represented by a striped box; sORF I and sORF II are indicated. (B) Analysis of the GC content of the *Mtenod40* gene. The sequence upstream of the transcription start site shows an average GC content of 40% (dashed line), which is equivalent to the isochore of the *Medicago* genome. However, the cDNA sequence has an average GC content of 50% (dashed line). (C) Stability analysis of the *enod40* genes. *enod40* transcripts were scanned for predicted RNA structures (windows from 30 to 300 bp; increment, 2 bp), and the number of standard deviations ($n\sigma$: value indicating the dispersion of the free energy of folding for each window, as described in reference 12) was calculated. Selected scans corresponding to specific window sizes (around 40 bp) are depicted for four *enod40* transcripts: *Mtenod40* (accession number X80264) for *M. truncatula*; *Trenod40* for *Trifolium repens* (accession number AJ000268); *Gmenod40* for *Glycine max* (accession number X69154), and *Osenod40* for *Oryza sativa* (accession number AB024054; nucleotides 2200 to 2642 corresponding to transcript 22). Regions containing highly stable predicted RNA structures measured by a high $n\sigma$ are indicated with an arrowhead. Bars indicate the position of conserved nucleotide sequences 1 and 2 in the different transcripts.

Nod factors induce cortical cell division. Division frequencies in our assay were comparable to those obtained by microtargeting chitin oligosaccharides or Nod factors (26, 36). Both the need to transduce a secondary signal from superficial cell layers where particles land into responsive cells in the inner cortex and the instability of the *enod40* gene products are expected to lower this value. In order to analyze the effects of the bombarded constructs, we studied responses induced only 2 days after bombardment. Longer times may introduce further variables (e.g., light conditions or hormonal changes during development). Apparently, *enod40* is not an inducer of cell division per se, but other factors likely present only in the inner cortex are required to complete cell cycle activation. Stable constitutive expression of *enod40* in transgenic plants resulted in a large proportion of dividing root cortical cells when grown under nitrogen-limited conditions (9) as well as accelerated nodulation (10), further suggesting that our transient assay is related to the biological activity of *enod40* in the root cortex.

enod40 is unusual in that it contains many sORFs, and the two peptides whose translation controls biological activity are encoded as such, in contrast to other eukaryotic small peptides, which are produced by cleavage of larger precursors containing signal sequences or related features (plant examples include systemin [32] and phytosulfokines [27]). Several reports suggest that plants do make use of peptides as signals in development, since both peptidic signals and putative receptors for them have been found (reviewed in reference 3). Moreover, mutations in these receptors influenced plant differentiation (2, 41). In our biological assay, however, we could not detect an effect of the synthetic peptide corresponding to sORF I (our unpublished results). The peptide may require certain modifications to become active, as has been shown for the phytosulfokine peptide growth factor (27). sORF-encoded small peptides may be able to diffuse out of the cell to act extracellularly, or alternatively, they may have intracellular targets that could be reached directly after translation. This is the case for the 5-amino-acid-encoding sORF in the 23S rRNA in *E. coli*, where the pentapeptide likely is produced and immediately binds its intracellular target, the rRNA (39). Several examples of the *cis* effects of upstream sORFs on 3′ translation mediated through binding to ribosomes have also been reported (25, 29) in eukaryotic cells. In these cases a 3′ long ORF codes for the protein having biological activity, in contrast to *enod40* genes, where only sORFs are found all along the transcript.

sORF-encoded peptides can be translated in plant tissues. We have previously proposed that *enod40* may code for a nontranslatable RNA (12). This was based on the fact that it lacked long ORFs, the computer-assisted prediction that it forms highly stable secondary structures, and the fact that it did not produce detectable in vitro translation products, properties shared with biologically active RNAs. In addition, the *enod40* RNA did not copurify with polysomes (1). In this work, however, using selected point mutants, we demonstrated that translation, size, and correct amino acid sequence of the 13-amino-acid sORF I as well as translation of sORF II are necessary for the biological activity of *enod40*. This supports the hypothesis that sORF-encoded peptides are biologically active, though we cannot exclude that translation from the *enod40* RNA may alter either the secondary structure or its decay or its capacity to interact with other proteins to form a ribonucleoprotein. sORF-encoded peptides may exert critical functions in sORF-RNAs through a variety of mechanisms (15, 25, 29, 43).

Localization of the peptide in the cell might help us in determining such a mechanism. Immunocompetition experiments indicated the presence of a domain related to the *enod40* sORF I-encoded peptide in alfalfa nodule extracts, in

agreement with previous experiments done in soybean (42). However, by using Western analysis or direct immunological approaches in alfalfa plants, we could not detect this *enod40* gene product even in young nodules, in which the transcript is very abundant. Oligopeptides are rapidly degraded in nodules and in vitro translation extracts, suggesting that immunological approaches may not be adequate to detect them biochemically. The high level of mRNA available for translation in the dividing cells of the nodule primordium may ensure continuous production of the oligopeptides in the cell via monosomes or a transient association with polysomes. Alternatively, the encoded peptides may be integrated into a larger protein complex (e.g., by coupling to an acceptor protein or a downstream sORF peptide) or into a structure (e.g., a ribonucleoprotein particle during translation), which could explain the presence of epitopes related to the *enod40* sORF I peptide in nodule extracts.

The recognition of the sORF I ATG was demonstrated both in vivo using reporter gene fusions and in vitro by translation of a larger peptide. The soybean sORF I was also shown to be translated in tobacco protoplasts using a green fluorescent protein reporter gene (42). Our translational analysis indicated that sORFs do not prevent reinitiation at downstream AUG codons in either differentiated epidermal and cortical cells or nondifferentiated cultured cells. The different *Mtenod40* sORFs are therefore likely to be translated with variable efficiency. Several plant mRNAs contain upstream sORFs that reduce translation of ORFs further downstream (15, 25, 29, 43). This was also the case for sORF II translation, as shown here using point mutations of sORF I. Several mechanisms to translate consecutive or overlapping ORFs exist in plant viruses (reviewed in reference 15) and might also exist in plants, where a polycistronic mRNA has recently been found (16). Even though sORFs are not generally considered gene products, our work indicates that both sORFs are required for *enod40* function, and hence it acts as a polycistronic transcript.

A puzzling result is that replacement of sORF I by the homologous sORF I of soybean yielded an inactive derivative. This revealed a certain level of "species specificity" for sORF I regulation of *enod40* action in alfalfa roots. A specific amino acid sequence might be required for appropriate function, suggesting that even nonconserved amino acids of the small peptide may play roles in target recognition. Strict sequence specificity of upstream sORFs has also been shown in translational regulation in mammalian cells (29).

Two regions of *Mtenod40* are functionally connected. Our data indicate that the action of sORF II depends on the translation of sORF I and this regulation is lost in the deleted *Mtenod40* derivative spanning the 3′ region (Δ5). In addition, this control is exerted not only at the level of translation, since either the altered size or the absence of sORF I had negative effects on *enod40* biological activity but decreased or increased sORF II translation, respectively. In these experiments, we also cannot exclude that interactions of the bombarded constructs with the endogenous alfalfa *enod40* gene occurred, affecting either its transcription or translation. However, no *enod40* mutant legume is yet available to analyze such an effect.

It has been proposed that the sORF I-encoded ENOD40 peptide is the active gene product and that the 3′ region might control its translation (even in *trans* on the endogenous gene 42). However, we could not detect activity of the *enod40* peptide in plant tissues, and the work based on a tobacco protoplast assay (42) could not be reproduced (35). This model cannot explain the effects of several point mutations that we detected as affecting *Mtenod40* activity in alfalfa roots. These mutations may perturb either the transcript stability or the capacity of the RNA to interact with the ribosomes or other intracellular target, having an indirect effect on *enod40* function. Hence, we think that the identified regions and sORFs are more likely required for determining the subcellular site where *enod40* is translated. This regulation can be overcome when using the deleted versions spanning only the sORF regions. Interestingly, RNA signals present in the 3′ untranslated regions of several genes have been shown to be involved in localization of mRNA translation (30), a feature that may be essential when the encoded gene products are unstable (such as the *enod40* oligopeptides). An alternative hypothesis is that sORF-mediated translational control of the transcript may also be exerted to allow stability or export of the RNA into the cytoplasm (as shown in animals [19]). Finally, the translation process per se might impose certain properties on the *enod40* mRNA. Nevertheless, we think that our experiments using the complete transcript are likely to reflect appropriately *enod40* gene regulation in vivo, since shorter forms of the *enod40* transcript have not been detected in planta.

Microtargeting of the sORF I or sORF II region alone is sufficient for *enod40* activity, whereas the inter-ORF region is inactive. This region, presenting predicted stable RNA structures, may determine transcript localization or stability. Alternatively, the critical parameter might be the correct spacing between sORFs that is also affected by the deletion of this region. Further studies on the involvement of RNA structures in gene function might await more sensitive methods to assay *enod40* activity. A predicted highly structured RNA region related to that of *Mtenod40* was detected in almost all *enod40* cDNAs found in the databases except for the tobacco gene. In this case, only a PCR product has been cloned, and we cannot exclude that this RNA structure is not required in this nonlegume plant or that the cloned fragment corresponded to a nonfunctional gene. Despite the large sequence variation detected in the inter-ORF region between *enod40* genes, it seems that a conserved stem structure could be detected even in the distantly related nonlegume rice plant. The predicted RNA structures were folded using an appropriate window according to the maximum $n\sigma$ value (Fig. 7). By comparing the two highly related sequences of *Trifolium repens* and *M. truncatula*, a compensatory mutation seemed to be present in the stem RNA region (arrow), further reinforcing the validity of the presence of an RNA structure in the *enod40* transcripts. Hence, this inter-ORF region, even though probably not directly responsible for gene function, seems to be involved in *enod40* gene regulation.

sORF translation and structured RNA signals might be important elements in the regulation of genes lacking long ORFs, particularly those having functions related to growth and differentiation, as shown here for *enod40* regulation in nodule organogenesis. Further analysis of the mechanism of *enod40* action in development [such as the identification of putative receptors or targets for the peptide(s) and/or structured RNA

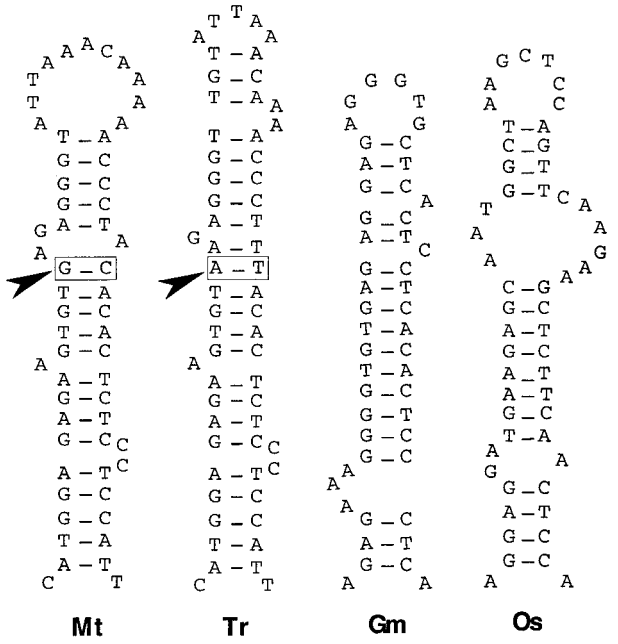

FIG. 7. Proposed RNA structures from different *enod40* transcripts. The regions presenting the highest $n\sigma$ in the different scans depicted in Fig. 6C were folded using MFOLD. A putative stem structure conserved in the *enod40* genes of the different species is proposed. The squares (arrow) indicate the presence of a compensatory mutation in the *Trenod40* and *Mtenod40* genes. Mt, *M. truncatula*; Tr, *T. repens*; Gm, *G. max*; Os, *O. sativa*.

region, as well as their subcellular localization] may uncover novel means of translational control of the cell.

ACKNOWLEDGMENTS

We thank Elke Fenner for technical assistance, H. Küster for providing pGUS-INT, Y. D'Aubenton-Carafa and C. Thermes for RNA structure analysis and helpful discussions, and L. Troussard for sequencing help.

C.J. was supported by a postdoctoral fellowship from the Swedish Council for Forestry and Agricultural Research and an EEC PTP training fellowship, C. Sousa by a postdoctoral fellowship from the EEC (TMR Marie Curie training grant), C.C. by a fellowship from the Ministère Français de l'Enseignement Supérieur et de la Recherche, and H.M. by a short-term EMBO fellowship.

REFERENCES

1. **Asad, S., Y. Fang, K. L. Wycoff, and A. M. Hirsch.** 1994. Isolation and characterization of cDNA and genomic clones of MsENOD40; transcripts are detected in meristematic cells of alfalfa. Protoplasma **183:**10–23.
2. **Becraft, P. W., P. S. Stinard, and D. R. McCarty.** 1996. CRINKLY4: a TNFR-like receptor kinase involved in maize epidermal differentiation. Science **273:**1406–1409.
3. **Bisseling, T.** 1999. The role of plant peptides in intercellular signalling. Curr. Opin. Plant Biol. **2:**365–368.
4. **Blondon, F., D. Marie, S. Brown, and A. Kondorosi.** 1994. Genome size and base composition in *Medicago sativa* and *M. truncatula* species. Genome **37:**264–275.
5. **Bonneville, J. M., H. Sanfaçon, J. Fütterer, and T. Hohn.** 1989. Post-transcriptional trans-activation in cauliflower mosaic virus. Cell **59:**1135–1143.
6. **Bullock, W. O., J. M. Fernández, and J. M. Short.** 1987. XL-1 Blue: a high efficiency plasmid-transforming *recA Escherichia coli* strain with beta-galactosidase selection. BioTechniques **5:**376–379.
7. **Burleigh, S. H., and M. J. Harrison.** 1997. A novel gene whose expression in *Medicago truncatula* roots is suppressed in response to colonization by vesicular-arbuscular mycorrhizal (VAM) fungi and to phosphate nutrition. Plant Mol. Biol. **34:**199–208.
8. **Cech, T. R., and B. L. Bass.** 1986. Biological catalysis by RNA. Annu. Rev. Biochem. **55:**599–629.
9. **Charon, C., C. Johansson, E. Kondorosi, A. Kondorosi, and M. Crespi.** 1997. *enod40* induces dedifferentiation and division of root cortical cells in legumes. Proc. Natl. Acad. Sci. USA **94:**8901–8906.
10. **Charon, C., C. Sousa, M. Crespi, and A. Kondorosi.** 1999. Alteration of *enod40* expression modifies *Medicago truncatula* root nodule development induced by *Sinorhizobium meliloti*. Plant Cell **11:**1953–1965.
11. **Corich, V., S. Goormachtig, S. Lievens, M. van Montagu, and M. Holsters.** 1998. Patterns of ENOD40 gene expression in stem-borne nodules of *Sesbania rostrata*. Plant Mol. Biol. **37:**67–76.
12. **Crespi, M. D., E. Jurkevitch, M. Poiret, Y. d'Aubenton-Carafa, G. Petrovics, E. Kondorosi, and A. Kondorosi.** 1994. *enod40*, a gene expressed during nodule organogenesis, codes for a non-translatable RNA involved in plant growth. EMBO J. **13:**5099–5112.
13. **Fang, Y., and A. M. Hirsch.** 1998. Studying early nodulin gene *ENOD40* expression and induction by nodulation factor and cytokinin in transgenic alfalfa. Plant Physiol. **116:**53–68.
14. **Furini, A., C. Koncz, F. Salamini, and D. Bartels.** 1997. High level transcription of a member of a repeated gene family confers dehydration tolerance to callus tissue of *Craterostigma plantagineum*. EMBO J. **16:**3599–3608.
15. **Fütterer, J., and T. Hohn.** 1996. Translation in plants—rules and exceptions. Plant Mol. Biol. **132:**159–189.
16. **García-Rios, M., T. Fujita, P. C. LaRosa, R. D. Locy, J. M. Clithero, R. A. Bressans, and L. N. Csonka.** 1997. Cloning of a polycistronic cDNA from tomato encoding γ-glutamyl phosphate reductase. Proc. Natl. Acad. Sci. USA **94:**8249–8254.
17. **Hanahan, D.** 1983. Studies on transformation of *Escherichia coli* with plasmids. J. Mol. Biol. **166:**557–580.
18. **Hao, Y., T. Crenshaw, T. Moulton, E. Newcomb, and B. Tycko.** 1993. Tumour-suppressor activity of H19 RNA. Nature **365:**764–767.
19. **Hentze, M., and A. Kulozik.** 1999. A perfect message: RNA surveillance and non-sense mediated decay. Cell **96:**307–310.
20. **Herrero, M., V. de Lorenzo, and K. T. Timmis.** 1990. Transposon vectors containing non-antibiotic selection markers for cloning and stable chromosomal insertion of foreign DNA in gram-negative bacteria. J. Bacteriol. **172:**6557–6567.
21. **Kouchi, H., and S. Hata.** 1993. Isolation and characterization of novel cDNAs representing genes expressed at early stages of soybean nodule development. Mol. Gen. Genet. **238:**106–119.
22. **Kouchi, H., K. Takane, R. So, J. Ladha, and P. Reddy.** 1999. Rice *ENOD40*: isolation and expression analysis in rice and transgenic soybean root nodules. Plant J. **18:**121–129.
23. **Leibovitch, M. P., V. C. Nguyen, M. S. Gross, B. Solhonne, S. A. Leibovitch, and A. Bernheim.** 1991. The human ASM (adult skeletal muscle) gene: expression and chromosomal assignment to 11p5*. Biochem. Biophys. Res. Commun. **180:**1241–1250.
24. **Leighton, P. A., R. S. Ingram, J. Eggenschwiler, A. Efstratiadis, and S. M. Tilghman.** 1995. Disruption of imprinting caused by deletion of the H19 gene region in mice. Nature **375:**34–39.
25. **Lovett, P. S., and E. J. Rogers.** 1996. Ribosomal regulation by the nascent peptide. Microbiol. Rev. **60:**366–385.
26. **Mathesius, U., H. R. M. Schlaman, H. P. Spaink, J. J. Weinman, C. Sautter, B. G. Rolfe, and M. A. Djordjevic.** 1998. Auxin transport inhibition precedes root nodule formation in white clover roots and is regulated by flavonoids and derivatives of chitin oligosaccharides. Plant J. **14:**23–34.
27. **Matsubayashi, Y., and Y. Sakagami.** 1996. Phytosulfokine, sulfated peptides that induce the proliferation of single mesophyll cells of *Asparagus officinalis* L. Proc. Natl. Acad. Sci. USA **93:**7623–7627.
28. **Minami, E., H. Kouchi, J. R. Cohn, T. Ogawa, and G. Stacey.** 1996. Expression of the early nodulin, *ENOD40*, in soybean roots in response to various lipo-chitin signal molecules. Plant J. **10:**23–32.
29. **Mize, G. J., H. Ruan, J. Low, and D. Morris.** 1998. The inhibitory upstream open reading frame from mammalian S-adenosyl methionine decarboxylase mRNA has a strict sequence specificity in critical positions. J. Biol. Chem. **273:**32500–32505.
30. **Oleynikov, Y., and R. Singer.** 1998. RNA localization: different zipcodes, same postman? Trends Cell Biol. **8:**381–383.
31. **Olivas, W. M., D. Muhlrad, and R. Parker.** 1997. Analysis of the yeast genome: identification of new non-coding and small ORF-containing RNAs. Nucleic Acids Res. **25:**4619–4625.
32. **Pearce, G., D. Strydom, S. Johnson, and C. A. Ryan.** 1991. A polypeptide from tomato leaves induces wound-inducible proteinase inhibitor proteins. Science **253:**895–898.
33. **Sambrook, J., E. F. Fritsch, and T. Maniatis.** 1989. Molecular cloning: a laboratory manual, 2nd ed. Cold Spring Harbor Laboratory Press, Cold Spring Harbor, N.Y.
34. **Sautter, C., H. Waldner, G. Neuhaus-Url, A. Galli, G. Neuhaus, and I. Potrykus.** 1991. Micro-targeting: high efficiency gene transfer using a novel approach for the acceleration of micro-projectiles. Biotechnology **9:**1080–1085.
35. **Schell, J., T. Bisseling, M. Dulz, H. Franssen, K. Fritze, M. John, T. Kleinow, A. Lessnick, E. Miklashevichs, K. Pawlowski, H. Rohrig, K. van de Sande, J. Schmidt, H. Steinbiss, and M. Stoll.** 1999. Re-evaluation of phytohormone-

independent division of tobacco protoplast-derived cells. Plant J. **17:**461–466.
36. **Schlaman, H. R. M., A. A. Gisel, N. E. M. Quaedvlieg, G. V. Bloemberg, B. J. J. Lugtenberg, J. W. Kijne, I. Potrykus, H. P. Spaink, and C. Sautter.** 1997. Chitin oligosaccharides can induce cortical cell division in roots of *Vicia sativa* when delivered by ballistic microtargeting. Development **124:** 4887–4895.
37. **Schultze, M., and A. Kondorosi.** 1998. Regulation of symbiotic root nodule development. Annu. Rev. Genet. **32:**33–57.
38. **Tam, W., D. Ben-Yehuda, and W. S. Hayward.** 1997. *bic*, a novel gene activated by proviral insertions in avian leukosis virus-induced lymphomas, is likely to function through its noncoding RNA. Mol. Cell. Biol. **17:**1490–1502.
39. **Tenson, T., A. DeBlasio, and A. Mankin.** 1996. A functional peptide encoded in the *Escherichia coli* 23S rRNA. Proc. Natl. Acad. Sci. USA **93:**5641–5646.
40. **Teramoto, H., T. Toyama, G. Takeba, and H. Tsuji.** 1996. Noncoding RNA for CR20, a cytokinin-repressed gene of cucumber. Plant Mol. Biol. **32:**797–808.
41. **Torii, K. U., N. Mitsukawa, T. Oosumi, Y. Matsuura, R. Yokoyama, R. F. Whittier, and Y. Komeda.** 1996. The Arabidopsis *ERECTA* gene encodes a putative receptor protein kinase with extracellular leucine-rich repeats. Plant Cell **8:**735–746.
42. **van de Sande, K., K. Pawlowski, I. Czaja, U. Wieneke, J. Schell, J. Schmidt, R. Walden, M. Matvienko, J. Wellink, A. van Kammen, H. Franssen, and T. Bisseling.** 1996. Modification of phytohormone response by a peptide encoded by *ENOD40* of legumes and a nonlegume. Science **273:**370–373.
43. **Wang, L., and S. Wessler.** 1998. Inefficient reinitiation is responsible for upstream open reading frame-mediated translational repression of the maize R gene. Plant Cell **10:**1733–1745.
44. **Yamashita, A., Y. Watanabe, N. Nukina, and M. Yamamoto.** 1998. RNA-assisted nuclear transport of the meiotic regulator Mei2p in fission yeast. Cell **95:**115–123.
45. **Yang, W. C., P. Katinakis, P. Hendriks, A. Smolders, F. de Vries, J. Spee, A. van Kammen, T. Bisseling, and H. Franssen.** 1993. Characterization of *GmENOD40*, a gene showing novel patterns of cell-specific expression during soybean nodule development. Plant J. **3:**573–585.
46. **Yoshida, H., H. Kumimoto, and K. Okamoto.** 1994. *dutA* RNA functions as an untranslatable RNA in the development of *Dictyostelium discoideum*. Nucleic Acids Res. **22:**41–46.